Journal of Food Measurement and Characterization (2024) 18:3458–3473
https://doi.org/10.1007/s11694-024-02417-w

ORIGINAL PAPER

Citric acid cross-linked biopolymeric nanofibers containing *Zataria multiflora* extract, an environmentally friendly active food packaging system

Leila Tayebi[1] · Fereshteh Bayat[1] · Arash Mahboubi[1] · Mohammad Kamalinejad[2] · Azadeh Haeri[1,3]

Received: 27 October 2023 / Accepted: 30 January 2024 / Published online: 18 March 2024

Abstract
The production of biodegradable food packaging has gained a great deal of attention due to the environmental concerns associated with the accumulation of plastic waste. In this study, chitosan (Cs)/gelatin (Gel) nanofibers (NFs) containing *Zataria multiflora* extract (ZME) were prepared through the electrospinning technique. Morphological characteristics of NFs were determined by scanning electron microscopy (SEM). NFs were cross-linked via a green process using citric acid and heat treatment. The effect of NF cross-linking on the structure, water stability, and mechanical behavior of the scaffolds was investigated. The antibacterial effectiveness of the prepared mats was studied by the colony counting method. In addition, the scaffolds were applied in the preservation of edible mushrooms. SEM analysis revealed smooth and bead-free Gel70-Cs30-ZME NFs with an average diameter of 188 nm. Cross-linked NFs possessed higher water contact angle (0° vs. 65.9°), swelling degree (45% vs. 1079%), and mechanical properties (tensile strength of 0.14 MPa vs. 0.45 MPa) than as-spun mats. Weight loss and water vapor permeability were reduced after cross-linking from 96 to 34% and from 6.7 to 5.2 g mm/kPa h m^2, respectively. Cross-linked Gel70-Cs30-ZME NFs exhibited satisfactory antibacterial activity with about 3 and 2 Log CFU/mL reduction of *Staphylococcus aureus* and *Escherichia coli* populations, respectively. Electrospun mats delayed the deterioration of mushrooms in comparison with the commonly used polyethylene films. Therefore, cross-linked Gel70-Cs30-ZME scaffold with improved mechanical and functional properties has potential applications in fruit and vegetable packaging.

✉ Azadeh Haeri
a_haeri@sbmu.ac.ir

[1] Department of Pharmaceutics and Pharmaceutical Nanotechnology, School of Pharmacy, Shahid Beheshti University of Medical Sciences, PO Box: 14155-6153, Tehran, Iran

[2] Department of Pharmacognosy, School of Pharmacy, Shahid Beheshti University of Medical Sciences, Tehran, Iran

[3] Protein Technology Research Center, Shahid Beheshti University of Medical Sciences, Tehran, Iran

Graphical abstract

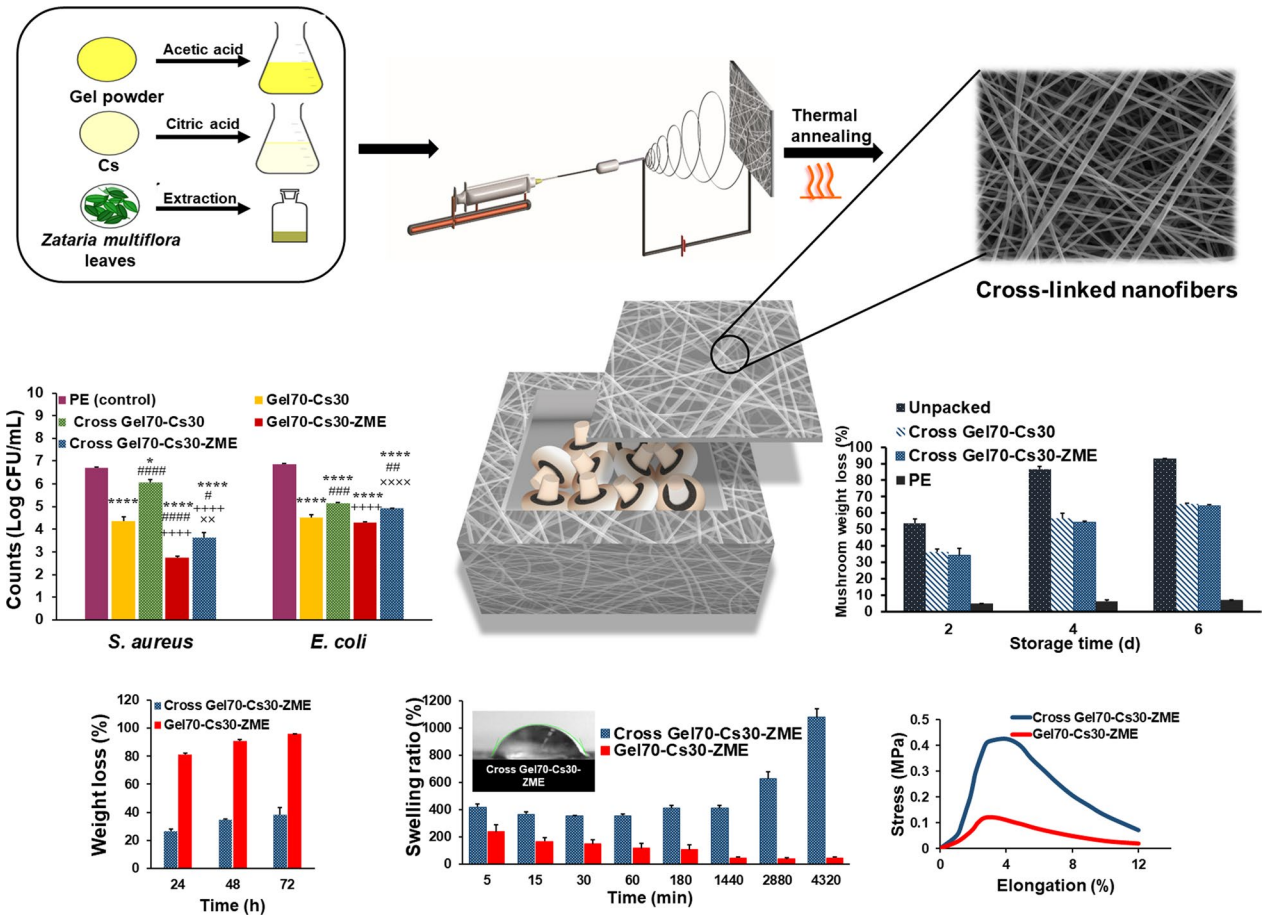

Keywords Nanofibers · Cross-linked · *Zataria multiflora* extract · Food packaging · Mushroom · Antimicrobial

Abbreviations

ANOVA	Analysis of variance
CFU	Colony-forming unit
Cs	Chitosan
E. coli	*Escherichia coli*
FTIR	Fourier transform infrared
GAE	Gallic acid equivalent
Gel	Gelatin
GRAS	Generally recognized as safe
MHA	Mueller Hinton agar
NFs	Nanofibers
PE	Polyethylene plastic film
PTCC	Persian type culture collection
PVA	Polyvinyl alcohol
QE	Quercetin equivalent
RF	Retardation factor
RH	Relative humidity
S. aureus	*Staphylococcus aureus*
SEM	Scanning electron microscopy
TFC	Total flavonoid content
TPC	Total phenolic content
WCA	Water contact angle
WVP	Water vapor permeability
ZM	*Zataria multiflora*
ZME	*Zataria multiflora* extract

Introduction

Food is affected by environmental conditions such as moisture, oxygen, and microorganisms, therefore, packaging is an important factor in the food industry to maintain the quality and safety of food [1]. Conventional packaging based on plastic materials is widely used. But the waste from these non-degradable packaging materials has caused serious environmental pollution. In recent years, research has focused on biopolymer-based packaging as a green technology. Biopolymers from natural resources (including

polysaccharides, proteins, and lipids) are biodegradable and environmentally friendly and can be used as alternatives to plastics [2, 3]. Moreover, microbial contamination is one of the main causes of food spoilage. Thus, the application of active packaging with antimicrobial properties has become popular [4].

Electrospinning is a versatile, simple, and cost-effective technique for fabricating fibers with nano- to micrometer diameters. Electrospun nanofibers (NFs) with nanoporous structure and high surface-to-volume ratio exhibit a high loading capacity and sustained release of bioactive substances. Therefore, NFs have been investigated as promising active food packaging systems [5–7]. Green tea essential oils loaded polycaprolactone/casein NFs [6] and zein/polylactic acid/hydroxypropyl methylcellulose NFs containing zenian (*Carum copticum*) [5] were recently studied as potential food packaging materials. Furthermore, Wu et al. prepared gelatin (Gel)/zein NFs loaded with cinnamaldehyde and thymol as an active food packaging system [8]. However, in some of these reports, the application of food preservation was not studied [5, 6].

The combination of Gel and chitosan (Cs) has been studied for the electrospinning of NFs [9]. Gel is a widely used protein biopolymer due to its bioavailability, biocompatibility, non-toxicity, low cost, and abundance. It has many applications in the pharmaceutical, food, and biomedical industries [10, 11]. Cs, a cationic polysaccharide, is obtained from the deacetylation of chitin, which is extracted from crustacean waste. In addition to biocompatibility and biodegradability, Cs has excellent antibacterial properties which make it a desirable candidate for active food packaging applications [12, 13]. In this regard, Cs casted film incorporated with tannic acid [14] and Cs/polyvinyl alcohol (PVA) NFs containing 1,8-cineole [15] were investigated as active food packaging.

The combination of Gel and Cs was chosen in this study due to the high spinnability of Gel [16] and the outstanding antimicrobial properties of Cs [12]. However, the as-spun nanofibrous mats without any modification are water-soluble and disintegrate immediately after exposure to aqueous media [17]. On the other hand, high mechanical strength and moisture resistance are essential for food packaging materials. Cross-linking is an effective method to provide these properties [1]. Using glutaraldehyde has been reported for cross-linking of carboxymethyl cellulose/Gel casted films [18] and Cs/PVA NFs [19]. Commonly used cross-linkers such as glutaraldehyde and genipin are toxic and expensive and therefore a safe alternative is required [20, 21]. Citric acid is a non-toxic, abundant, and inexpensive tricarboxylic acid which is naturally found in citrus fruits. Covalent amide bonds are formed between the carboxyl groups of citric acid and amino groups of Cs during heat treatment [22, 23]. Citric acid has been applied for cross-linking of Cs NFs in a few studies [24, 25]. The use of citric acid as a green crosslinker in nanofibrous food packaging is a novel strategy and very limited studies have been conducted in this field [26, 27] and none of these studies have been done on Cs/Gel NFs. To the best of our knowledge, using citric acid for cross-linking of Cs/Gel nanofibrous packaging was explored in this study for the first time.

Zataria multiflora (ZM), a member of Lamiaceae, is a thyme-like herb that is used for the management of cough, bronchitis, and irritable bowel syndrome and also as a flavoring spice. Furthermore, several studies have shown the antibacterial, antifungal, antioxidant, and anti-inflammatory activities of ZM. Thymol and carvacrol are the major components of ZM [28]. These phenolic monoterpenes are classified as Generally Recognized As Safe (GRAS) by FDA and possess broad-spectrum antimicrobial properties [29]. Moreover, Mahboubi et al. have reported the antibacterial activity of ZM hydroalcoholic extract (ZME) against four important foodborne pathogens [30]. Mohammadi et al. showed the antimicrobial activity of sage seed gum casted film containing ZM as a potential food packaging system [31]. In another study, Cs/ZM coating enhanced the shelf life of salmon fish [32]. Abdollahi-Kazeminezhad et al. prepared antibacterial polyvinylpyrrolidone/kafirin NFs activated by ZM essential oil as a potential food packaging system [33]. However, to the best of our knowledge, there is no study conducted on citric acid cross-linked ZM activated nanofibrous food packaging. In other words, the combination of Cs, Gel, citric acid and ZM was conducted for the first time in the current paper.

In this article, citric acid cross-linked Cs/Gel NFs containing ZME were successfully fabricated by the electrospinning technique. The developed NFs were characterized using scanning electron microscopy (SEM) and Fourier transform infrared (FTIR) analysis. The water contact angle (WCA), swelling degree, weight loss, mechanical properties, and water vapor permeability (WVP) were also studied. The antibacterial activity of NFs was evaluated using the colony counting method. Finally, the efficiency of the electrospun mat in the preservation of fresh mushrooms was investigated. Therefore, the combination of Gel, Cs, and ZME, with synergistic antibacterial activity in the form of NFs is expected to be suitable for application in food packaging.

Materials and methods

Materials

Chitosan (Cs) (medium Mw), gelatin (Gel), citric acid, acetic acid, sodium carbonate, Folin–Ciocalteu reagent, gallic acid, quercetin, kaempferol, toluene, ethyl acetate, formic acid, and aluminum chloride ($AlCl_3$) were obtained from

Merck/Sigma-Aldrich (Germany). ZM was purchased from a local grocery store and identified by the Department of Pharmacognosy, School of Pharmacy, Shahid Beheshti University of Medical Sciences, Tehran, Iran under the voucher number SBMU-8024. All the chemicals were of analytical grade and purchased from Merck/Sigma-Aldrich (Germany). Bacterial strains were obtained from the Persian Type Culture Collection (PTCC) (Tehran, Iran).

Preparation of the extract

ZME was prepared using the maceration method [30]. 100 g of dried and crushed leaves of ZM were macerated in 2 L of 50% ethanol for 3 days. The extract was filtered and concentrated to dryness using a 90 °C water bath over about 24 h. ZME was stored at 4 °C for further experiment.

Total phenolic content (TPC)

The Folin Ciocalteu technique was selected to assess the TPC of ZME using gallic acid as standard as previously reported [34] with slight modification. 1 mL of diluted Folin–Ciocalteu reagent (1:10 with deionized water) was mixed with 200 µL of ZME in the test tube. After 10 min, 0.8 mL of sodium carbonate (7% w/v) was added to the mixture and the test tube was allowed to stand for 30 min in total darkness. Shimadzu UVmini-1240 spectrophotometer was used to measure the absorbance of the sample at 760 nm. The results were indicated as mg of gallic acid equivalent (GAE)/g of ZME.

Total flavonoid content (TFC)

Aluminum chloride colorimetric assay was employed to determine the TFC of ZME [34] with minor changes. Briefly, 1 mL of ZME and 1 mL of different concentrations (5–40 µg/mL) of quercetin as standard solutions were transferred to test tubes and 1 mL of 2% w/v $AlCl_3$ was added to each solution. After 40 min of incubation, the absorbance of the samples was monitored at 420 nm. TFC of ZME was determined from the calibration plot of quercetin concentration vs absorbance and reported as mg of quercetin equivalent (QE)/g of ZME.

High-performance thin-layer chromatography (HPTLC) fingerprint analysis

HPTLC analysis was performed to identify and quantify kaempferol in ZME [35]. Different volumes of the kaempferol standard solution, corresponding to kaempferol concentrations of 0.11, 0.22, 0.55, 0.99, and 1.1 mg/mL, were used to plot the calibration curve. The various kaempferol concentrations and 1 µL of ZME were spotted on the HPTLC plate as 10.0 mm bands. CAMAG automatic TLC sampler 4 (ATS4) equipped with a 25 µL syringe was utilized to apply the samples. Samples were positioned 10.0 mm from the bottom edge, 25.0 mm from the side edge, and 13.6 mm apart from each other. The plate development was carried out in an ascending mode in a twin-trough glass chamber using 10 mL of mobile phase. The mobile phase consisted of a mixture of toluene, ethyl acetate, and formic acid (6:4:0.3). The migration distance of the mobile phase was 90 mm during the analysis. Afterward, the plate was removed from the chamber and dried at 60 °C for 5 min. The plate was scanned using CAMAG TLC scanner 3 at the wavelength of 365 nm, using an absorbance mode. The source of the radiation employed was a deuterium lamp. The slit dimensions, data resolution, and scanning speed were 5.00 × 0.30 mm, 100 mm/step, and 20 mm/s, respectively.

Preparation of the solutions

Firstly, the Cs solution (3.5% w/w) was prepared by dissolving Cs in 0.2 M citric acid and stirred at 55 °C for 3 h and then at room temperature overnight. Gel powder was dissolved in 50% (v/v) acetic acid under stirring at 45 °C for 4 h to obtain a 30% (w/w) solution. Then the Gel and Cs solutions were mixed (at 100:0, 80:20, 70:30, and 60:40 weight ratios) for 24 h at room temperature. ZME was added to the solutions at a weight ratio of 1:10 (ZME:polymer) and mixed for an additional 1 h to obtain Gel α-Cs β-ZME solutions, where α and β represent the weight percentage of Gel and Cs solutions, respectively.

Electrospinning process

An electrospinning apparatus (Nanoazma, Iran) was used for the fabrication of NFs. Gel-Cs-ZME solutions were displaced into a 5 mL plastic syringe with a 23G steel needle. The mixtures were pumped at a flow rate of 0.20 mL/h. The collection distance and applied voltage were fixed at 15 cm and 19 kV, respectively. All of the spinning operations were performed at room temperature.

Surface morphology and diameter determination

The morphology of NFs was observed using MIRA3 FE-SEM (TESCAN, Czech Republic) field emission SEM. Each sample of prepared NFs was sputter-coated with gold. Based on the SEM images, the diameters of 50 NFs were measured using ImageJ analysis software. Based on the results, Gel70-Cs30-ZME NFs were chosen for further evaluation.

Cross-linking of nanofibrous scaffolds

Gel70-Cs30 (fibers without ZME) and Gel70-Cs30-ZME NFs were placed in a hot air oven and heated at 120 °C for 6 h to perform the cross-linking reaction, according to the method described by Pangon et al. for PVA/Cs NFs [36] and were coded as Cross Gel70-Cs30 and Cross Gel70-Cs30-ZME, respectively.

NFs characterization

Water resistance analysis

SEM was applied to monitor the structural integrity of the as-spun and cross-linked mats. For this purpose, NFs were placed into aqueous media for 15 and 30 min, followed by SEM evaluation.

Water contact angle (WCA)

The hydrophilicity and wettability of the as-spun and cross-linked scaffolds were analyzed with a contact angle measurement system. A droplet of distilled water (5 µL) was dropped at three different places on the NFs surface and the average of these three measurements was reported.

Swelling ratio

The nanofibrous mats (15 × 15 mm) were weighed (W1) and immersed in distilled water for predetermined periods. Samples were then collected and weighed (W2) after removing the surface liquid using filter paper. The swelling ratio was calculated by the following equation [36]:

$$\text{Swelling ratio}(\%) = \frac{W2 - W1}{W1} \times 100$$

Weight loss

The nanofibrous mats were weighed (W1) and immersed in distilled water for 24, 48, and 72 h. The samples were then dried at room temperature for 24 h and weighed again (W2). Weight loss was calculated using the following formula [36]:

$$\text{Weight loss}(\%) = \frac{W1 - W2}{W1} \times 100$$

Water vapor permeability (WVP)

WVP tests of NFs carried out according to the gravimetric method [37]. NFs samples were sealed on the top of the cups containing distilled water, leaving little space between the water surface and NFs mats. Thus, one side of the nanofibrous mats was exposed to 100% relative humidity (RH) inside the cup. The test cups were then placed in a glass desiccator with dried silica gel at 25 °C. The weight of cups was measured every 24 h over 4 days. WVP was determined as follows [37]:

$$WVP = \frac{FL}{\mathrm{A}\Delta\mathrm{p}}$$

where F is the slope of weight loss versus time (g/h) graph, L is the film thickness (mm), A is the test area (cup mouth area (m^2)), and Δp is the partial vapor pressure difference between the two sides of the nanofibrous mat (kPa).

Mechanical properties

The mechanical properties of the samples were determined using STM-20, SANTAM universal test machine, Iran. Samples were tested using a load cell of 500 N and crosshead speed of 1 mm/min to obtain stress–strain curves.

Fourier transform infrared (FTIR)

A WQF-510 FTIR spectrometer (Rayleigh Analytical Instrument Corporation, China) was used to analyze the molecular interactions and functional groups of pure materials and prepared NFs within a range of 4000–400 cm^{-1} and resolution of 4 cm^{-1}.

Functional properties of NFs

Antibacterial activities

The agar well diffusion method was used to investigate the antibacterial properties of ZME [38]. Two bacterial strains (*Staphylococcus aureus* (*S. aureus*), ATCC 25923, and *Escherichia coli* (*E. coli*), ATCC 25922) were selected for this study. Mueller Hinton agar (MHA) plates were inoculated with 100 µL of bacterial suspensions of 1.5×10^8 colony-forming units (CFU)/mL. An 8 mm diameter well was aseptically punched on the medium surface. 100 µL of different concentrations of ZME (diluted with distilled water) was added to each well, and then incubated at 35 °C for 24 h. After incubation, the zones of inhibition were assessed. All experiments were repeated three times.

The antibacterial activities of Gel70-Cs30, Gel70-Cs30-ZME, Cross Gel70-Cs30, and Cross Gel70-Cs30-ZME NFs were evaluated by the colony counting method [39] against *S. aureus* and *E. coli*. Polyethylene plastic film (PE) was used as the control. The NFs were cut into circular discs (24 mm in diameter) and sterilized under UV radiation for 40 min (20 min each side). 100 µL of bacterial suspension

(1.5×10^8 CFU/mL in normal saline) was pipetted on each sample and incubated for 24 h. Serial dilutions were made using normal saline and 1 mL of each solution was mixed with 15 mL of the nutrient agar medium in sterile plates and incubated at 35 °C for 24 h. Finally, the number of colonies was counted and reported as log (CFU)/mL.

Application of NFs for food packaging

Fresh mushrooms (*Agaricus bisporus*) were purchased from a local supermarket and assigned to four groups: the first group was packed with PE, the second and third groups were packed with Cross Gel70-Cs30 and Cross Gel70-Cs30-ZME NFs, respectively, and in the last group mushrooms were kept unpacked which were considered as the control. All samples were stored at 25 °C and observed periodically for their appearance, weight loss, and spoilage. The weight loss of mushrooms was calculated according to the following equation [40]:

$$\text{Weight loss}(\%) = \frac{W_i - W_t}{W_i} \times 100$$

W_i: the initial weight of mushrooms, W_t: weight of mushrooms at storage time.

Statistical analysis

All experiments were performed in triplicate and the results were presented as means ± standard error of mean. Data were analyzed by *t*-test and one-way analysis of variance (ANOVA) (GraphPad Prism). Statistical significance was considered at a P value < 0.05.

Results

Total phenolic and flavonoid contents and HPTLC of ZME

The yield of dried extract (ZME) was 21.8 g/100 g of dry ZM leaves. The TPC and TFC were 162.4 ± 2.2 mg GAE/g ZME and 21.7 ± 0.3 mg QE/g ZME, respectively. HPTLC analysis was also performed (Fig. 1a). To identify kaempferol, the retardation factor (Rf) of the compound in the sample were compared to the standard. The matching Rf value confirmed the presence of kaempferol. The Rf of kaempferol was found to be 0.568 ± 0.002 (Fig. 1b). The calibration curve was linear in the range of 0.11–1.1 mg/mL ($y = 11.88x - 932.8$, $R^2 = 0.998$). The content of kaempferol in the extract was 2.52 mg/g herbal extract.

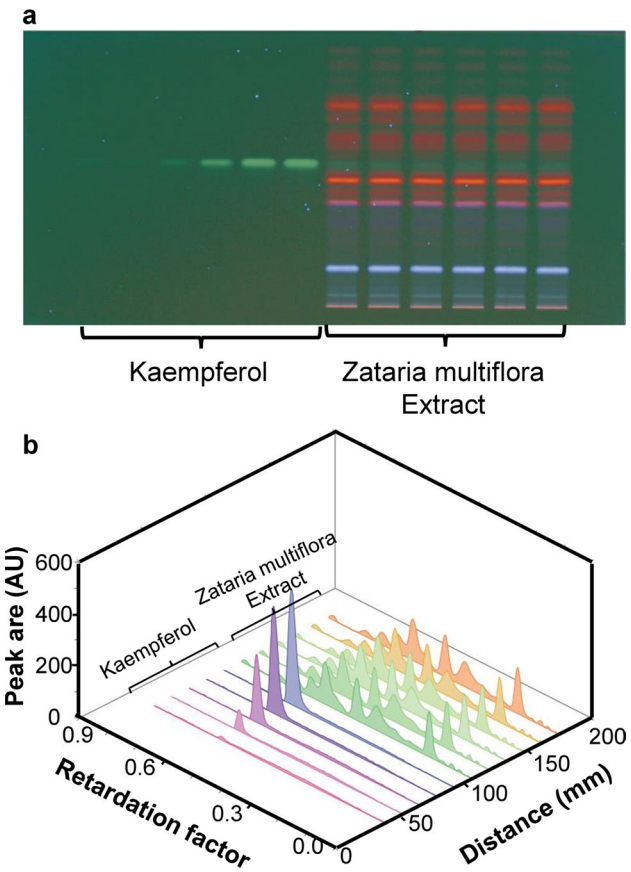

Fig. 1 **a** HPTLC profile of kaempferol (track 1–6) and ZME (track 7–12) on the silica plate at 365 nm and **b** the corresponding three-dimensional densitometric chromatogram of kaempferol standard solution (at different concentrations) and the herbal extract

Diameter and morphology of different Gel-Cs-ZME NFs

Figure 2a shows the SEM images of Gel100-Cs0-ZME, Gel80-Cs20-ZME, Gel70-Cs30-ZME, and Gel60-Cs40-ZME NFs. These photographs confirm the formation of NFs in all formulations. The first three formulations had uniform, smooth, and bead-free structures without any visible particles, indicating the compatibility between the ingredients and the integration of extract into the scaffolds. With an increase in Cs concentration to 40%, beads and defects were observed in Gel60-Cs40-ZME NFs.

The diameter distributions and the average fiber diameter of samples are presented in Fig. 2b and c. As can be seen, pure Gel NFs showed the highest average diameter (775 ± 12 nm). By increasing the Cs concentration to 30%, the average diameter of the NFs significantly decreased to 188 ± 7 nm (P < 0.0001 vs. Gel100-Cs0-ZME and Gel80-Cs20-ZME). There was no significant difference between the diameters of Gel70-Cs30-ZME and Gel60-Cs40-ZME NFs (P > 0.05).

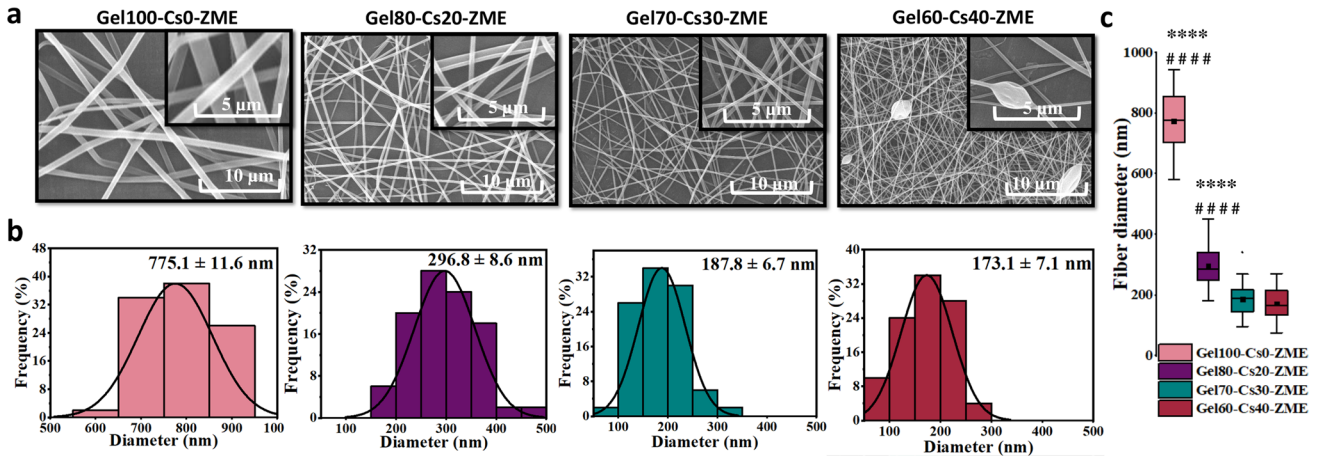

Fig. 2 SEM images (**a**) and diameter distribution and average diameter (**b**) of as-spun NFs with different Gel:Cs ratios; box and whisker plot for fiber diameters. Box boundaries represent 50% (25–75%) of all data points and the line inside is the median value (**c**). (**** and ####: $P < 0.0001$ vs. Gel70-Cs30-ZME and Gel60-Cs40-ZME NFs, respectively)

Cs can provide enormous functional properties for food packaging, including antibacterial and antioxidant activities [12]. Thus, NFs containing the highest amount of Cs as well as no morphological defects were desirable in this study. Therefore, Gel70-Cs30-ZME NFs were chosen as the optimum formulation.

Water resistance analysis

Figure 3 shows the morphological changes of Gel70-Cs30-ZME and Cross Gel70-Cs30-ZME NFs before and after water contact. Based on the results, the fibrous morphology of the Gel70-Cs30-ZME sample was completely lost after 15 min of water contact while cross-linked NFs retained their morphology and swelled during 30 min of water exposure.

WCA measurement

WCA indicates surface wettability [41]. It was observed that the water droplet on the as-spun mat disappeared immediately, which was attributed to the super hydrophilicity of the scaffold. In contrast, the cross-linked mat had a WCA value of 65.9 ± 3.4° (Fig. 4a) indicating the efficacy of the cross-linking process.

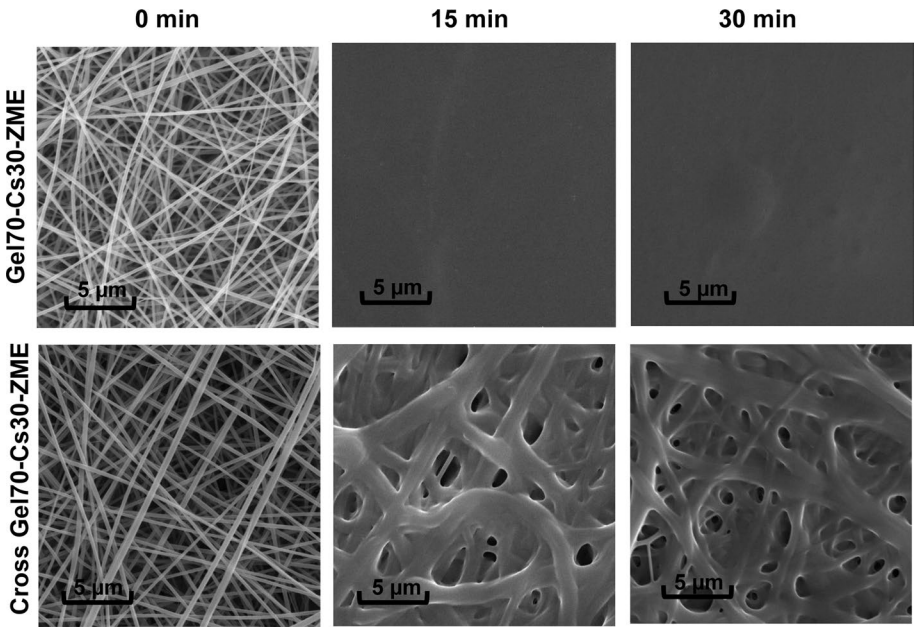

Fig. 3 SEM images of as-spun (top) and cross-linked (bottom) NFs before and after water contact for 15 and 30 min

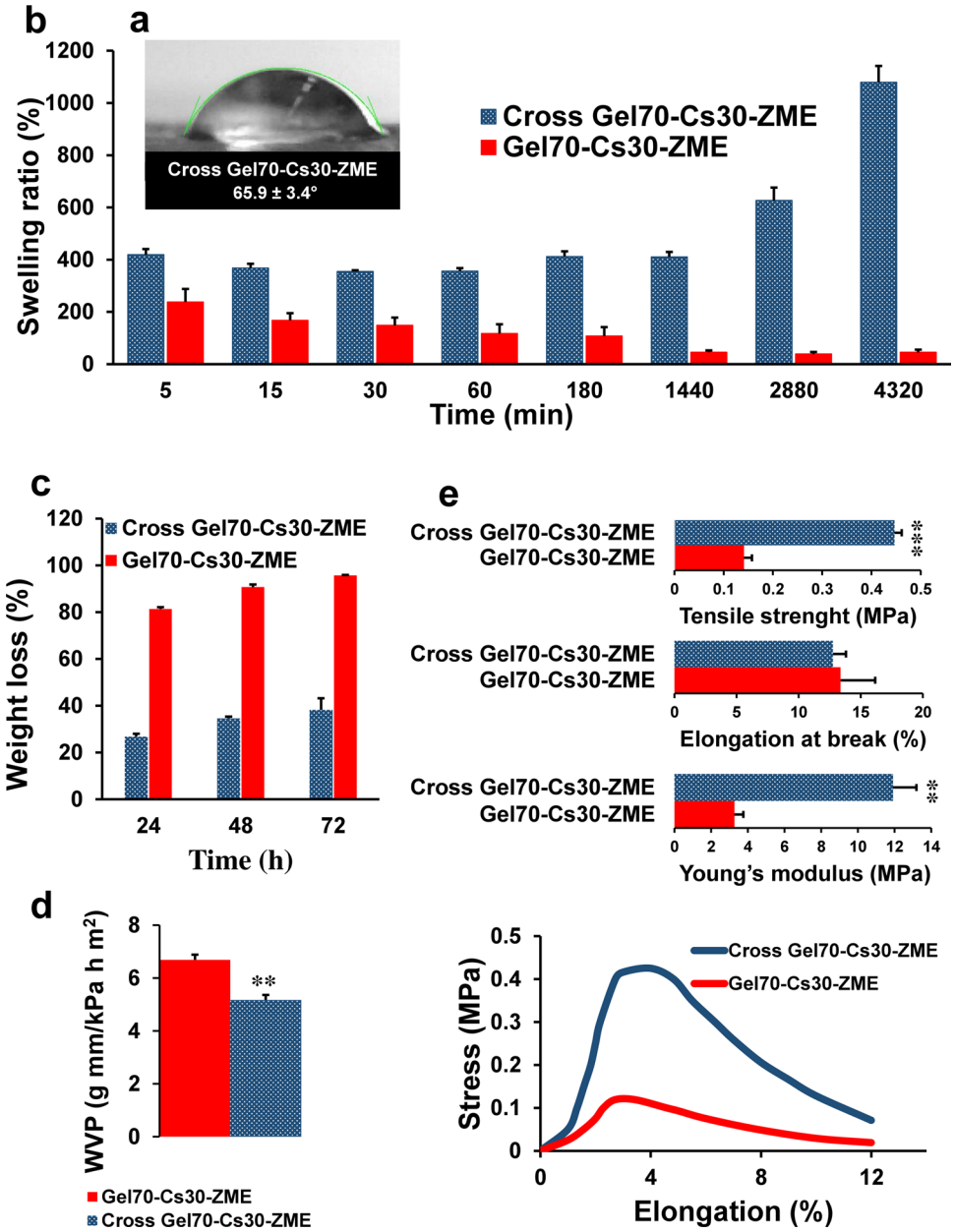

Fig. 4 WCA (**a**), swelling ratio (**b**), weight loss (**c**), WVP (**d**) and mechanical properties (**e**) of as-spun and cross-linked scaffolds. **: $P < 0.01$ and ***: $P < 0.001$ vs. Gel70-Cs30-ZME

Swelling ratio and weight loss analyses

Figure 4b illustrates the swelling patterns of Gel70-Cs30-ZME and Cross Gel70-Cs30-ZME NFs. As can be seen, the Cross Gel70-Cs30-ZME membrane showed a higher swelling ratio compared with Gel70-Cs30-ZME scaffold at all time points. The swelling degree increased from 419 ± 21% to 1079 ± 62% for cross-linked NFs and decreased from 238 ± 50% to 45 ± 10% over 72 h for as-spun mats.

The weight loss data of Gel70-Cs30-ZME and Cross Gel70-Cs30-ZME NFs are presented in Fig. 4c. As can be observed, the weight loss of the as-spun mat was 81% at 24 h, and increased over time to 96% at 72 h. The cross-linked scaffold exhibited an almost constant percentage of weight loss at all time points ($P > 0.05$, ~ 34%) which was significantly lower than that of the as-spun mat ($P < 0.001$ at all time points).

WVP measurement

One of the main functions of food packaging is limiting the transfer of water vapor between food and the environment and WVP reflects this ability of polymeric scaffolds [42]. As shown in Fig. 4d, Gel70-Cs30-ZME and Cross Gel70-Cs30-ZME NFs possessed the WVP value of 6.69 ± 0.20 g mm/kPa h m^2 and 5.17 ± 0.19 g mm/kPa h m^2, respectively ($P < 0.01$).

Mechanical properties

The influence of cross-linking by citric acid and heat treatment on the mechanical properties of NFs is presented in Fig. 4e. Tensile strength and Young's modulus of the cross-linked scaffold were about three and four times higher than that of the as-spun mat, respectively. The elongation at break of scaffolds remained unchanged after cross-linking ($P > 0.05$).

FTIR analysis

Figure 5a shows the FTIR spectra of pure Gel, Cs, ZME, citric acid, the physical mixture, and the prepared NFs. The FTIR spectrum of Gel powder showed characteristic bands at 1650 cm^{-1} (C=O stretching of amide I), 1547 cm^{-1} (N–H bending of amide II), and 1241 cm^{-1} (N–H bending of amide III). A broad peak located at around 3300 cm^{-1} was attributed to the N−H and O−H stretching vibrations [43, 44]. For Cs, a peak positioned at 3457 cm^{-1} corresponded to N−H and O−H stretching vibrations. The peak at 2918 cm^{-1} was related to C−H stretching. Peaks at 1653 and 1597 cm^{-1} belonged to C=O stretching (amide I) and N–H bending vibrations, respectively. The peak at 1078 cm^{-1} was attributed to C−O−C stretching [24, 43, 44]. ZME showed vibrations at 3422, 1600–1400, and 1253 cm^{-1} corresponding to phenolic groups, C=C−C of the aromatic ring, and aromatic ether, respectively [39]. For citric acid, the peak at 3284 cm^{-1} was attributed to O−H stretching. Two peaks at 1745 and 1691 cm^{-1} were associated with C=O stretching of carboxylic acid [45]. The FTIR spectrum of the physical mixture exhibited a superposition of the peaks of pure substances. In ZME-loaded NFs, stronger absorption bands at around 3400 and 1600–1400 cm^{-1} (especially at 1459 and 1418 cm^{-1}) confirmed the incorporation of ZME in NFs. Figure 5b shows the cross-linking mechanism of Cs by citric acid and heat treatment.

Antibacterial properties

Figure 6a shows the inhibition zones of different concentrations of ZME against *S. aureus* (the Gram-positive bacteria) and *E. coli* (the Gram-negative bacteria). ZME exhibited a concentration-related antibacterial activity against *S. aureus* (25 mg/mL: 10 mm, 100 mg/mL: 14 mm, and 400 mg/mL: 18 mm). No inhibition zone was observed for tested concentrations against *E. coli*.

The antibacterial activities of NFs are presented in Fig. 6b. As can be seen, Gel70-Cs30 NFs decreased the population of *S. aureus* around 2 Log CFU/mL, which is attributed to the antibacterial activity of Cs. The *S. aureus* count after treatment with Gel70-Cs30-ZME NFs was 2.75 Log CFU/mL which is about 2 and 4 Log CFU/mL lower than that of Gel70-Cs30 and control mats, respectively. This indicates the combined antibacterial properties of Cs and ZME. A comparison of bacterial populations treated with as-spun and cross-linked samples demonstrates that the cross-linking process reduces the antimicrobial effect.

In the case of *E. coli*, there was no significant difference between the bacterial populations treated with Gel70-Cs30 and Gel70-Cs30-ZME NFs. This result was also true for Cross Gel70-Cs30 and Cross

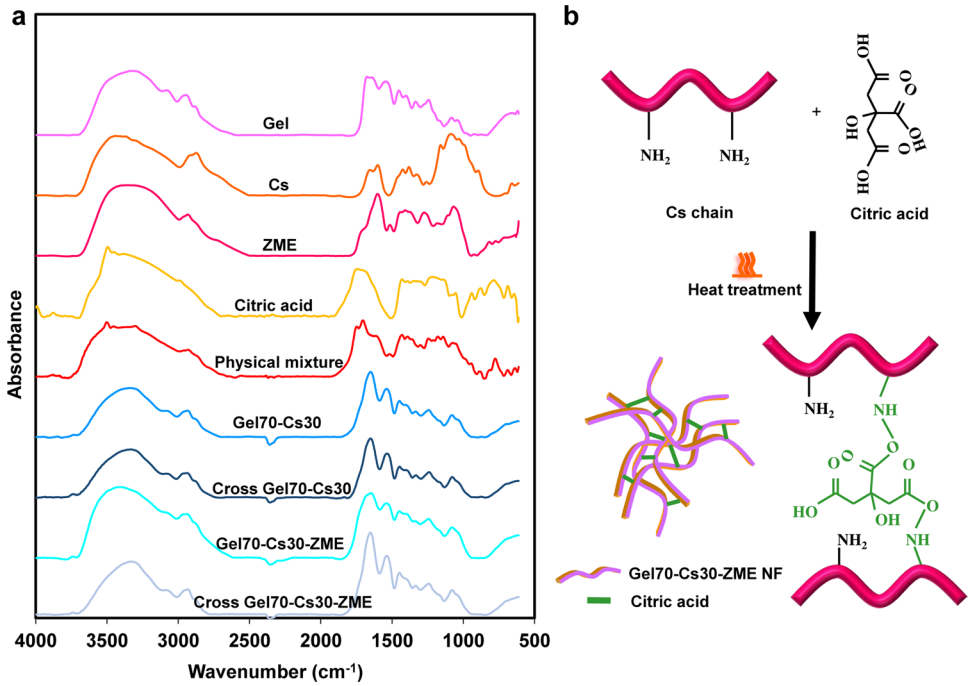

Fig. 5 FTIR spectrum of Gel, Cs, ZME, citric acid, the physical mixture, and different NFs (**a**), Schematic illustration of cross-linking reaction between Cs and citric acid through thermal annealing (**b**)

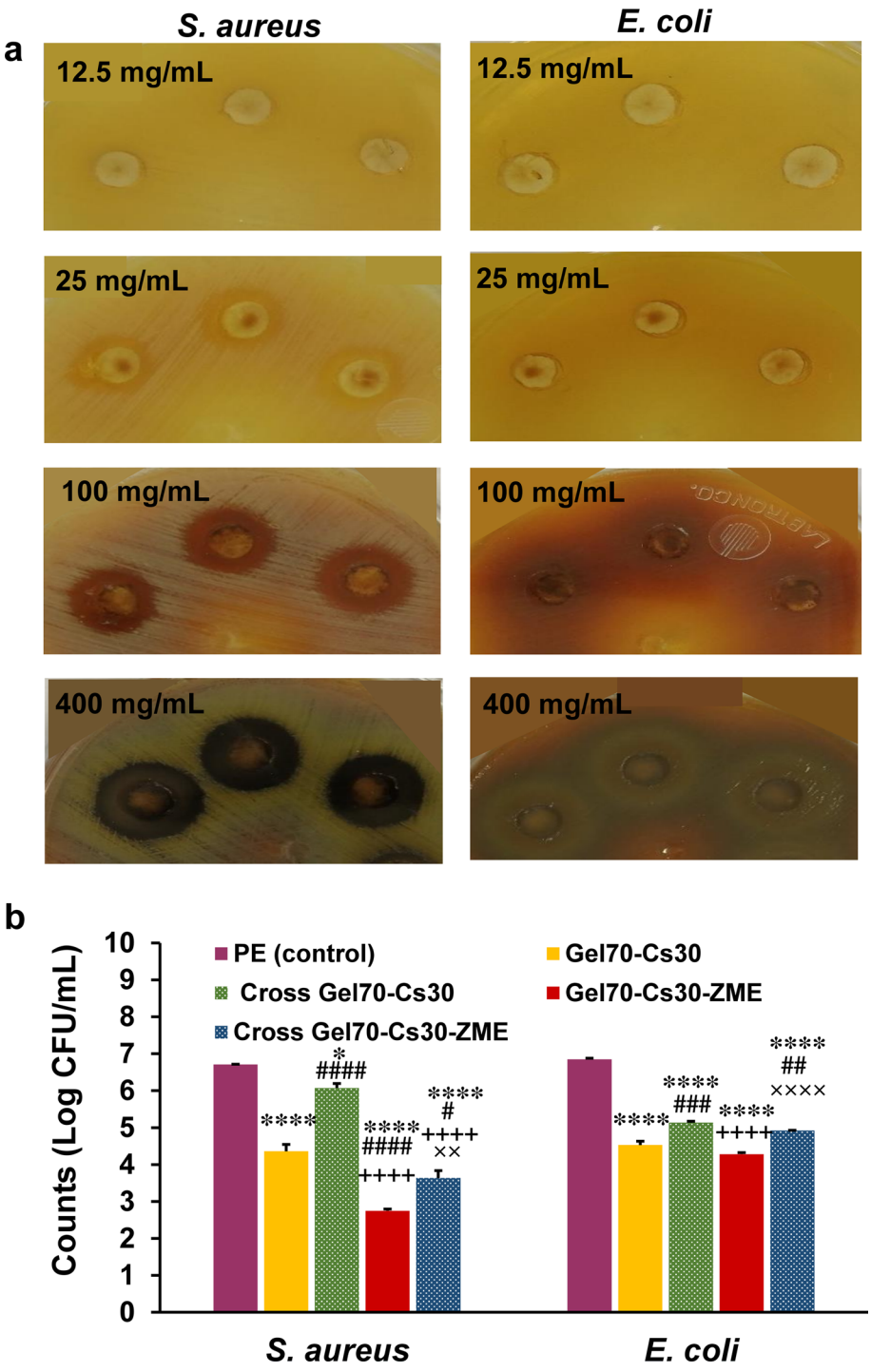

Fig. 6 Inhibition zones of different concentrations of ZME against *S. aureus* (left) and *E. coli* (right) (**a**); Effect of different mats on the growth of *S. aureus* and *E. coli* (**b**) (****: $P<0.0001$ and *: $P<0.05$ vs. PE, ####: $P<0.0001$, ###: $P<0.001$, ##: $P<0.01$ and #: $P<0.05$ vs. Gel70-Cs30, ++++: $P<0.0001$ vs Cross Gel70-Cs30, ××: $P<0.01$ and ××××: $P<0.0001$ vs. Gel70-Cs30-ZME.)

Gel70-Cs30-ZME samples and confirms the lack of antibacterial activity of ZME against *E. coli* (Fig. 6a). Nevertheless, the Cross Gel70-Cs30 scaffold was able to reduce the bacterial count by about 2 Log CFU/mL which was lower than the as-spun mats.

Mushroom preservation study

In the current study, the mechanical stability of NFs and their moisture resistance were enhanced after cross-linking. Therefore, Cross Gel70-Cs30 and Cross Gel70-Cs30-ZME

scaffolds were selected for evaluation of food preservation capacity.

The appearance of mushrooms packed with different samples during storage time is shown in Fig. 7a. According to the results, the unpacked mushrooms had a dry and wrinkled appearance, while the other samples maintained their freshness during 6 days of storage. As shown in Fig. 7a, the mold was observed on the stem of mushrooms covered with PE at 4th day. Thus, these mushrooms became inedible after 4 days. In contrast, the mushrooms packed with nanofibrous mats did not exhibit decay till the end of the experiment.

Figure 7b presents the weight loss values of mushrooms. According to the results, the weight loss of all samples increased by increasing the storage time. The highest and lowest weight loss values were recorded for unpacked and PE-treated mushrooms, respectively (93% and 7% at 6th day, respectively). A weight loss value of around 65% was obtained for mushrooms treated with Cross Gel70-Cs30 and Cross Gel70-Cs30-ZME NFs on day 6, which was significantly ($P < 0.0001$) lower than that of the control group.

Discussion

Nowadays, using biopolymers and natural active substances has been a topic of research interest in the field of food packaging due to their bioavailability, biocompatibility, and antimicrobial activity [3]. Despite these advantages, their

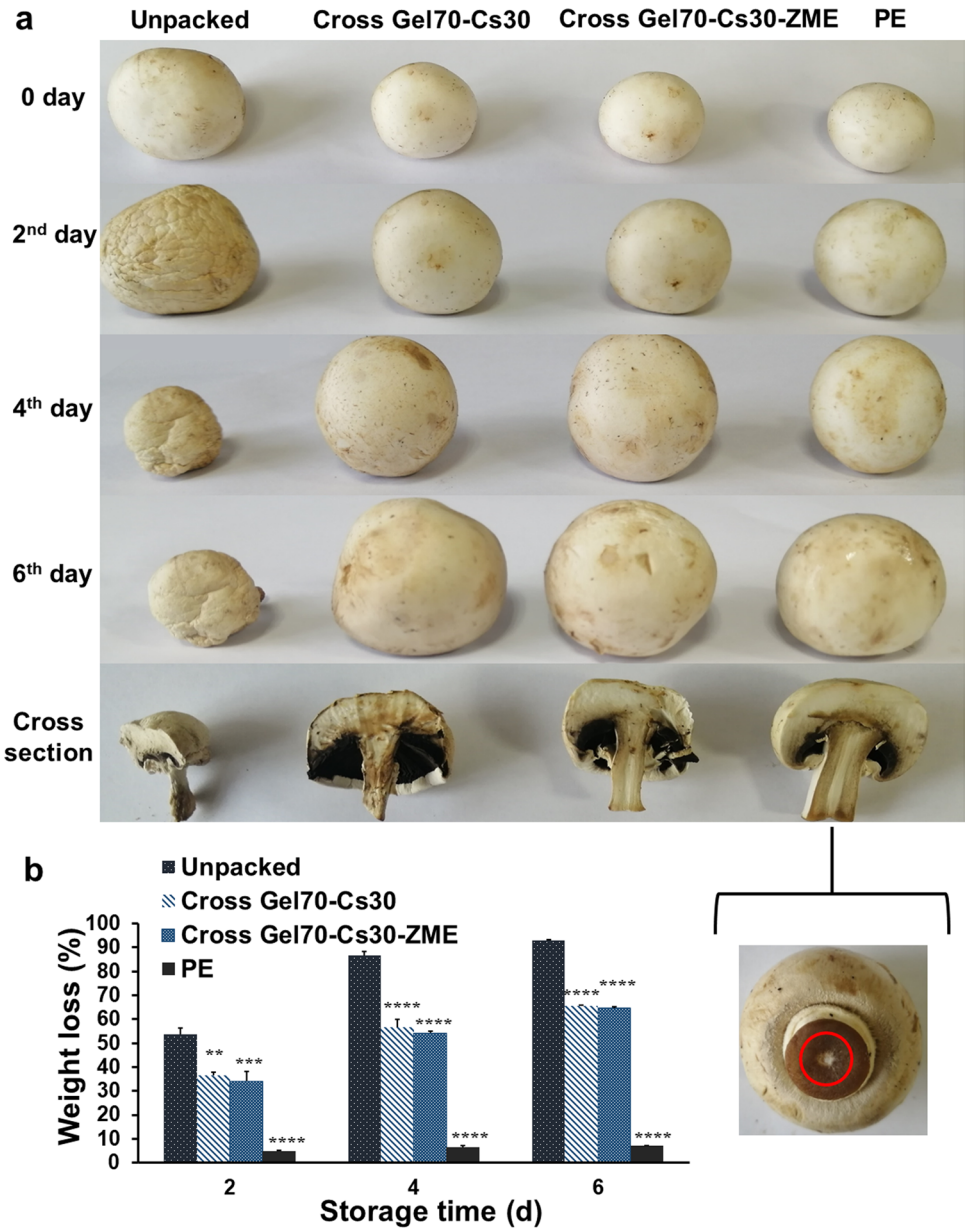

Fig. 7 Effect of different mats on appearance (**a**) and Weight loss (**b**) of mushrooms during storage time. (**: $P < 0.01$, ***: $P < 0.001$ and ****: $P < 0.0001$ vs. unpacked mushrooms)

application is limited because of low moisture stability and mechanical properties [1]. In this regard, our effort was to develop cross-linked Gel-Cs NFs containing antibacterial ZME, through a feasible and safe method, which does not require using any toxic cross-linkers.

ZM is rich in active polyphenols [28, 29]. Hence, the standardization of the extract was carried out by measuring total phenolic and flavonoid contents. Different amounts of polyphenols have been reported for ZME. Mahboubi et al. [30] and Fatemi et al. [46] reported lower TPC and higher TFC values, compared to the present study, respectively. These variations are mainly due to differences in environmental characteristics, climatic conditions, and the type of solvent used [47]. HPTLC is an analytical tool that separates, identifies, and quantifies chemical compounds of a sample in a single step. It is a rapid and relatively low-cost technique that requires small sample volumes and minimal mobile phase [48]. HPTLC fingerprint analysis was conducted to determine kaempferol in ZME. Kaempferol is one of the flavonoid components in ZME [49]. Based on the data, this component was found to be 2.52 mg/g in the herbal extract (Fig. 1).

The surface morphology and diameter size of NFs were determined with the aim of SEM analysis (Fig. 2). The presence of beads in NFs with higher Cs content has been reported previously [50]. The amine groups in the Cs structure become protonated in acidic solutions and a positively charged and highly viscous solution is obtained. As a result, the electrical field cannot overcome the surface tension on the tip of the jet. This phenomenon leads to the formation of beads and non-uniform NFs [50, 51]. Achieving thinner fibers due to higher Cs concentration is in agreement with the results of previous experiments performed on drug-free [52] and ε-polylysine loaded NFs [44]. The positive charge of Cs could lead to the high conductivity of the spinning solution and the fabrication of NFs with smaller diameters [44].

To verify the effectiveness of the cross-linking process some tests including SEM analysis after water contact (water resistance) (Fig. 3), WCA, swelling, weight loss, WVP, and mechanical analysis (Fig. 4) were operated. The enhancement of the water resistance of NFs after cross-linking (Fig. 3) has been observed previously in glutaraldehyde-mediated Cs /PVA NFs [53]. Similar to the present study, SEM images showed that the porous structure was preserved in cross-linked scaffolds while the as-spun ones lost their fibrous morphology after soaking in water which could indicate the partial dissolution of the polymer structure [53].

The WCA value reflects the surface wettability of nanofibrous membranes, which is affected by the chemical composition [41]. The WCA value of 0° has been reported for Gel/polycaprolactone [54] and Cs/polylactic acid NFs [55]. The increase in the surface hydrophobicity upon cross-linking may be attributed to the involvement of polar groups in the formation of hydrophobic ester bonds between Cs and citric acid (Fig. 5b), resulting in a higher WCA value [45].

The swelling degree is a sum of weight gain and weight loss of membranes upon immersion in water. The weight gain results from the stability of the 3D structure of the scaffold and its water-retaining capacity while weight loss occurs when the membrane is unstable and disintegrates in water [56]. In the present study, weight gain was the dominant phenomenon for cross-linked Gel70-Cs30-ZME NFs (Fig. 4b), which can be attributed to the enhanced water stability caused by cross-linking, while weight loss happened for uncross-linked NFs which may be due to their high water-solubility.

Weight loss analysis (Fig. 4c) reveals the stability of a membrane in aqueous media. In this study, the water stability of NFs increased dramatically after cross-linking, which is in agreement with the results of Pangon et al. that showed the as-spun Cs/PVA NFs containing different multicarboxylic acids dissolved completely in water, while the cross-linked mats exhibited a low percentage of weight loss [36]. This could be due to recombination and increased interaction between components through heat treatment cross-linking (Fig. 5b) [25].

Generally, low WVP values are preferred to extend the shelf life of packaged foods [12]. Similarly, Tayeb and Tajvidi reported a decrease in WVP of nanocellulose film using a cross-linking agent and heat treatment as a result of the esterification reaction between the components [57]. Besides, the cross-linking process makes the polymer chains more compact and reduces the diffusion of water molecules [58].

Since the electrospun membranes are prepared for food packaging application, they must be able to provide suitable mechanical properties during processing, transportation, and handling to maintain their integrity [1]. In the current study, the stiffness of the scaffolds was enhanced due to cross-linking (Fig. 4e). This may be due to the interaction and formation of strong bonding between components which makes the structure more compact [59]. Similar trends of increasing tensile strength and Young's modulus due to cross-linking by citric acid and heat treatment have been demonstrated for sesame protein membrane [59] and starch film [60]. In general, cross-linking reduces the elongation at break of scaffolds and makes them less flexible, which is not favorable in food packaging applications. However, in the case of citric acid, different and controversial results have been reported, which are attributed to the plasticizing effect of citric acid [1, 59, 60]. In this work, the absence of a significant difference between the elongation at break of the as-spun and cross-linked mats indicates that cross-linking with citric acid and thermal annealing did not decrease the flexibility and ductility of NFs.

FTIR analysis elucidates chemical interactions between active ingredients and polymers during the preparation process. The main peaks of the pure materials were similar to those documented in previous studies [39, 43–45]. In this study, no major difference was observed between the FTIR spectra of as-spun and cross-linked fibers (Fig. 5a). According to the cross-linking reaction, the effect of cross-linking on the FTIR spectrum is determined by the changes in peaks associated with amide I and II [25, 61]. These peaks were obscured by the characteristic peaks of Gel at these points.

Since microbial contamination is considered to be an important reason for food spoilage [4], Cs and ZME were used as antimicrobial agents in prepared NFs. The antibacterial studies of NFs (Fig. 6b) revealed that both as-spun and cross-linked Gel70-Cs30-ZME scaffolds could effectively reduce the populations of *S. aureus* and *E. coli*. Lower antibacterial activity in cross-linked scaffolds may be due to the interaction of functional groups of Cs during cross-linking process. In fact, the protonated amino groups of Cs polymer interact with the negatively charged molecules on the bacterial cell surface and cause the permeability and leakage of the intracellular material, resulting in bacterial cell death [12]. During heat treatment, amino groups interact with the citric acid and lead to the formation of covalent amide bonds [23]. Hence, these amino groups were unavailable and Cs cannot fully exert its antibacterial activity. Grkovic et al. fabricated cross-linked Cs/polyethylene oxide NFs using citric acid and thermal annealing. They showed that by increasing the heating temperature from 80 to 145 °C, the cross-linking improved while the antibacterial activity decreased due to the amino groups reduction [25].

To evaluate the application of NFs in food packaging, edible mushrooms were used (Fig. 7). The longer shelf life of mushrooms packed with NFs is presumably related to the antimicrobial properties of electrospun mats and prevention of moisture accumulation compared to PE. In a similar study, less spoilage of strawberries covered with NFs containing the antibacterial peptide nisin was attributed to the absorption of surface moisture and antibacterial activity of the NFs [62]. Dehydration is an important factor affecting the mushroom quality during its shelf life. In this study, a 28% reduction in weight loss value was achieved by packing the mushrooms with NFs in comparison with the control group (Fig. 7b). Similar results were also reported by Shao et al. when they coated edible mushrooms with zein NFs containing cinnamaldehyde essential oil [63].

Conclusion

In the current work, Gel/Cs NFs loaded with ZME were fabricated as an antibacterial food packaging material via the electrospinning technique. Citric acid was used as the cross-linking agent. Gel70-Cs30-ZME NFs were chosen as the optimum formulation due to the uniform and bead-free structure as observed by SEM. Thermal annealing was applied in order to complete the cross-linking reaction and prepare cross-linked NFs. Cross Gel70-Cs30-ZME NFs exhibited higher surface hydrophobicity and water vapor barrier property and lower solubility compared with the as-spun sample. The cross-linking process had a positive effect on the mechanical properties. Antimicrobial studies revealed that the ZME-loaded NFs could efficiently inhibit bacterial growth due to the presence of Cs and ZME. Besides, prepared NFs were effectively able to extend the shelf life of edible mushrooms. Considering the water resistance, mechanical and antibacterial properties, and food preservation ability, the novel Cross Gel70-Cs30-ZME electrospun membrane could be a potential candidate for food packaging application.

Author contributions Leila Tayebi: methodology, investigation, data curation, formal analysis, visualization, writing—original draft. Fereshteh Bayat: methodology, investigation, formal analysis, writing—original draft. Arash Mahboubi: conceptualization, methodology, supervision, writing—review & editing. Mohammad Kamalinejad: methodology, data curation, writing—review & editing. Azadeh Haeri: conceptualization, methodology, supervision, visualization, funding acquisition, writing—review & editing.

Funding This work was supported by the Shahid Beheshti University of Medical Sciences, Tehran, Iran (Grant No. 27562).

Data availability The datasets of the current study are available from the corresponding author upon reasonable request.

Declarations

Competing interests The authors declare no competing interests.

References

1. F. Garavand, M. Rouhi, S.H. Razavi, I. Cacciotti, R. Mohammadi, Improving the integrity of natural biopolymer films used in food packaging by crosslinking approach: a review. Int. J. Biol. Macromol. **104**, 687–707 (2017). https://doi.org/10.1016/j.ijbiomac.2017.06.093
2. A. Trajkovska Petkoska, D. Daniloski, N.M. D'Cunha, N. Naumovski, A.T. Broach, Edible packaging: sustainable solutions and novel trends in food packaging. Food Res. Int. **140**, 109981 (2021). https://doi.org/10.1016/j.foodres.2020.109981
3. M. Taherimehr, H. YousefniaPasha, R. Tabatabaeekoloor, E. Pesaranhajiabbas, Trends and challenges of biopolymer-based nanocomposites in food packaging. Compr. Rev. Food Sci. Food Saf. **20**, 5321–5344 (2021). https://doi.org/10.1111/1541-4337.12832
4. H.M.C. Azeredo, C.G. Otoni, D.S. Corrêa, O.B.G. Assis, M.R. de Moura, L.H.C. Mattoso, Nanostructured antimicrobials in food packaging-recent advances. Biotechnol. J. **14**, e1900068 (2019). https://doi.org/10.1002/biot.201900068
5. M. Aman Mohammadi, S. Ramezani, H. Hosseini, A.M. Mortazavian, S.M. Hosseini, M. Ghorbani, Electrospun antibacterial

and antioxidant zein/polylactic acid/hydroxypropyl methylcellulose nanofibers as an active food packaging system. Food Bioprocess Technol. **14**, 1529–1541 (2021). https://doi.org/10.1007/s11947-021-02654-7
6. L. Yavari Maroufi, S. PourvatanDoust, F. Naeijian, M. Ghorbani, Fabrication of electrospun polycaprolactone/casein nanofibers containing green tea essential oils: applicable for active food packaging. Food Bioprocess Technol. **15**, 2601–2615 (2022). https://doi.org/10.1007/s11947-022-02905-1
7. F. Topuz, T. Uyar, Antioxidant, antibacterial and antifungal electrospun nanofibers for food packaging applications. Food Res. Int. **130**, 108927 (2020). https://doi.org/10.1016/j.foodres.2019.108927
8. X. Wu, Z. Liu, S. He, J. Liu, W. Shao, Development of an edible food packaging gelatin/zein based nanofiber film for the shelf-life extension of strawberries. Food Chem. **426**, 136652 (2023). https://doi.org/10.1016/j.foodchem.2023.136652
9. I.H. Ali, A. Ouf, F. Elshishiny, M.B. Taskin, J. Song, M. Dong, M. Chen, R. Siam, W. Mamdouh, Antimicrobial and wound-healing activities of graphene-reinforced electrospun chitosan/gelatin nanofibrous nanocomposite scaffolds. ACS Omega **7**, 1838–1850 (2022). https://doi.org/10.1021/acsomega.1c05095
10. N. Sahoo, R.K. Sahoo, N. Biswas, A. Guha, K. Kuotsu, Recent advancement of gelatin nanoparticles in drug and vaccine delivery. Int. J. Biol. Macromol. **81**, 317–331 (2015). https://doi.org/10.1016/j.ijbiomac.2015.08.006
11. M.C. Echave, R. Hernáez-Moya, L. Iturriaga, J.L. Pedraz, R. Lakshminarayanan, A. Dolatshahi-Pirouz, N. Taebnia, G. Orive, Recent advances in gelatin-based therapeutics. Expert Opin. Biol. Ther. **19**, 773–779 (2019). https://doi.org/10.1080/14712598.2019.1610383
12. H. Wang, J. Qian, F. Ding, Emerging chitosan-based films for food packaging applications. J. Agric. Food Chem. **66**, 395–413 (2018). https://doi.org/10.1021/acs.jafc.7b04528
13. A. Muxika, A. Etxabide, J. Uranga, P. Guerrero, K. de la Caba, Chitosan as a bioactive polymer: processing, properties and applications. Int. J. Biol. Macromol. **105**, 1358–1368 (2017). https://doi.org/10.1016/j.ijbiomac.2017.07.087
14. S.J. Lee, M.A. Gwak, K. Chathuranga, J.S. Lee, J. Koo, W.H. Park, Multifunctional chitosan/tannic acid composite films with improved anti-UV, antioxidant, and antimicrobial properties for active food packaging. Food Hydrocoll. **136**, 108249 (2023). https://doi.org/10.1016/j.foodhyd.2022.108249
15. C. Cheng, T. Min, Y. Luo, Y. Zhang, J. Yue, Electrospun polyvinyl alcohol/chitosan nanofibers incorporated with 1,8-cineole/cyclodextrin inclusion complexes: characterization, release kinetics and application in strawberry preservation. Food Chem. **418**, 135652 (2023). https://doi.org/10.1016/j.foodchem.2023.135652
16. Z. Yang, S. Chaieb, Y. Hemar, Gelatin-based nanocomposites: a review. Polym. Rev. **61**, 765–813 (2021). https://doi.org/10.1080/15583724.2021.1897995
17. K. Jalaja, D. Naskar, S.C. Kundu, N.R. James, Potential of electrospun core-shell structured gelatin-chitosan nanofibers for biomedical applications. Carbohydr. Polym. **136**, 1098–1107 (2016). https://doi.org/10.1016/j.carbpol.2015.10.014
18. A. Zafar, M.K. Khosa, A. Noor, S. Qayyum, M.J. Saif, Carboxymethyl cellulose/gelatin hydrogel films loaded with zinc oxide nanoparticles for sustainable food packaging applications. Polymers **14**, 5201 (2022). https://doi.org/10.3390/polym14235201
19. N. Rosli, W.Z.N. Yahya, M.D.H. Wirzal, Crosslinked chitosan/poly(vinyl alcohol) nanofibers functionalized by ionic liquid for heavy metal ions removal. Int. J. Biol. Macromol. **195**, 132–141 (2022). https://doi.org/10.1016/j.ijbiomac.2021.12.008
20. M. Bilal, I. Gul, A. Basharat, S.A. Qamar, Polysaccharides-based bio-nanostructures and their potential food applications. Int. J. Biol. Macromol. **176**, 540–557 (2021). https://doi.org/10.1016/j.ijbiomac.2021.02.107
21. D. Rocha-García, A. Guerra-Contreras, J. Reyes-Hernández, G. Palestino, Thermal and kinetic evaluation of biodegradable thermo-sensitive gelatin/poly(ethylene glycol) diamine crosslinked citric acid hydrogels for controlled release of tramadol. Eur. Polym. J. **89**, 42–56 (2017). https://doi.org/10.1016/j.eurpolymj.2017.02.007
22. S.H. Lee, P. Md Tahir, W.C. Lum, L.P. Tan, P. Bawon, B.-D. Park, S.S. Osman Al Edrus, U.H. Abdullah, A review on citric acid as green modifying agent and binder for wood. Polymers **12**, 1692 (2020). https://doi.org/10.3390/polym12081692
23. J. Khouri, A. Penlidis, C. Moresoli, Viscoelastic properties of crosslinked chitosan films. Processes (2019). https://doi.org/10.3390/pr7030157
24. M. Sazegar, S. Bazgir, A.A. Katbab, Preparation and characterization of water-absorbing gas-assisted electrospun nanofibers based on poly(vinyl alcohol)/chitosan. Mater. Today Commun. **25**, 101489 (2020). https://doi.org/10.1016/j.mtcomm.2020.101489
25. M. Grkovic, D.B. Stojanovic, V.B. Pavlovic, M. Rajilic-Stojanovic, M. Bjelovic, P.S. Uskokovic, Improvement of mechanical properties and antibacterial activity of crosslinked electrospun chitosan/poly(ethylene oxide) nanofibers. Composites B. **121**, 58–67 (2017). https://doi.org/10.1016/j.compositesb.2017.03.024
26. S. Estevez-Areco, L. Guz, R. Candal, S. Goyanes, Release kinetics of rosemary (*Rosmarinus officinalis*) polyphenols from polyvinyl alcohol (PVA) electrospun nanofibers in several food simulants. Food Packag. Shelf Life **18**, 42–50 (2018). https://doi.org/10.1016/j.fpsl.2018.08.006
27. S. Estevez-Areco, L. Guz, R. Candal, S. Goyanes, Development of insoluble PVA electrospun nanofibers incorporating R-limonene or β-cyclodextrin/R-limonene inclusion complexes. J. Polym. Environ. **30**, 2812–2823 (2022). https://doi.org/10.1007/s10924-022-02390-9
28. H. Sajed, A. Sahebkar, M. Iranshahi, *Zataria multiflora* Boiss. (Shirazi thyme)—an ancient condiment with modern pharmaceutical uses. J. Ethnopharmacol. **145**, 686–698 (2013). https://doi.org/10.1016/j.jep.2012.12.018
29. K. Kachur, Z. Suntres, The antibacterial properties of phenolic isomers, carvacrol and thymol. Crit. Rev. Food Sci. Nutr. (2019). https://doi.org/10.1080/10408398.2019.1675585
30. A. Mahboubi, M. Kamalinejad, A.M. Ayatollahi, M. Babaeian, Total phenolic content and antibacterial activity of five plants of Labiatae against four foodborne and some other bacteria. Iran. J. Pharm. Res. **13**, 559–566 (2014). https://doi.org/10.22037/ijpr.2014.1504
31. M. Mohammadi, R. Yekta, H. Hosseini, F. Shahraz, S.M. Hosseini, S. Shojaee-Aliabadi, A. Mohammadi, Characterization of a novel antimicrobial film based on sage seed gum and *Zataria multiflora* Boiss essential oil. J. Food Meas. Charact. **17**, 167–177 (2023). https://doi.org/10.1007/s11694-022-01509-9
32. N. Zomorodian, S. Javanshir, N. Shariatifar, S. Rostamnia, The effect of essential oil of *Zataria multiflora* incorporated chitosan (free form and pickering emulsion) on microbial, chemical and sensory characteristics in salmon (*Salmo trutta*). Food Chem. X **20**, 100999 (2023). https://doi.org/10.1016/j.fochx.2023.100999
33. N. Abdollahi-Kazeminezhad, M. Esmaiili, H. Almasi, H. Hamishehkar, Fabrication and characterization of antimicrobial hybrid electrospun polyvinylpyrrolidone/kafirin nanofibers activated by *Zataria multiflora* essential oil. J. Food Meas. Charact. **17**, 4850–4863 (2023). https://doi.org/10.1007/s11694-023-01998-2
34. S. Khan, T. Khan, A.J. Shah, Total phenolic and flavonoid contents and antihypertensive effect of the crude extract and fractions of *Calamintha vulgaris*. Phytomedicine **47**, 174–183 (2018). https://doi.org/10.1016/j.phymed.2018.04.046

35. H. Panchal, A. Amin, M. Shah, Development of validated high-performance thin-layer chromatography method for simultaneous determination of quercetin and kaempferol in *Thespesia populnea*. Pharmacogn. Res. **9**, 277–281 (2017). https://doi.org/10.4103/0974-8490.210326
36. A. Pangon, S. Saesoo, N. Saengkrit, U. Ruktanonchai, V. Intasanta, Multicarboxylic acids as environment-friendly solvents and in situ crosslinkers for chitosan/PVA nanofibers with tunable physicochemical properties and biocompatibility. Carbohydr. Polym. **138**, 156–165 (2016). https://doi.org/10.1016/j.carbpol.2015.11.039
37. Y. Zou, C. Zhang, P. Wang, Y. Zhang, H. Zhang, Electrospun chitosan/polycaprolactone nanofibers containing chlorogenic acid-loaded halloysite nanotube for active food packaging. Carbohydr. Polym. **247**, 116711 (2020). https://doi.org/10.1016/j.carbpol.2020.116711
38. S.H. Salmen, S.A. Alharbi, Silver nanoparticles synthesized biogenically from *Aloe fleurentiniorum* extract: characterization and antibacterial activity. Green Chem. Lett. Rev. **13**, 1–5 (2020). https://doi.org/10.1016/10.1080/17518253.2019.1707883
39. N.T. Ardekani, M. Khorram, K. Zomorodian, S. Yazdanpanah, H. Veisi, H. Veisi, Evaluation of electrospun poly(vinyl alcohol)-based nanofiber mats incorporated with *Zataria multiflora* essential oil as potential wound dressing. Int. J. Biol. Macromol. **125**, 743–750 (2019). https://doi.org/10.1016/j.ijbiomac.2018.12.085
40. Y. Liu, Y. Yuan, S. Duan, C. Li, B. Hu, A. Liu, D. Wu, H. Cui, L. Lin, J. He, W. Wu, Preparation and characterization of chitosan films with three kinds of molecular weight for food packaging. Int. J. Biol. Macromol. **155**, 249–259 (2020). https://doi.org/10.1016/j.ijbiomac.2020.03.217
41. R.S. Kurusu, N.R. Demarquette, Surface modification to control the water wettability of electrospun mats. Int. Mater. Rev. **64**, 249–287 (2019). https://doi.org/10.1080/09506608.2018.1484577
42. H. Hu, X. Yao, Y. Qin, H. Yong, J. Liu, Development of multifunctional food packaging by incorporating betalains from vegetable amaranth (*Amaranthus tricolor* L.) into quaternary ammonium chitosan/fish gelatin blend films. Int. J. Biol. Macromol. **159**, 675–684 (2020). https://doi.org/10.1016/j.ijbiomac.2020.05.103
43. S. Gomes, G. Rodrigues, G. Martins, C. Henriques, J.C. Silva, Evaluation of nanofibrous scaffolds obtained from blends of chitosan, gelatin and polycaprolactone for skin tissue engineering. Int. J. Biol. Macromol. **102**, 1174–1185 (2017). https://doi.org/10.1016/j.ijbiomac.2017.05.004
44. F. Liu, Y. Liu, Z. Sun, D. Wang, H. Wu, L. Du, D. Wang, Preparation and antibacterial properties of ε-polylysine-containing gelatin/chitosan nanofiber films. Int. J. Biol. Macromol. **164**, 3376–3387 (2020). https://doi.org/10.1016/j.ijbiomac.2020.08.152
45. H. Wu, Y. Lei, J. Lu, R. Zhu, D. Xiao, C. Jiao, R. Xia, Z. Zhang, G. Shen, Y. Liu, S. Li, M. Li, Effect of citric acid induced crosslinking on the structure and properties of potato starch/chitosan composite films. Food Hydrocoll. **97**, 105208 (2019). https://doi.org/10.1016/j.foodhyd.2019.105208
46. F. Fatemi, Y. Asri, I. Rasooli, D. Alipoor Sh, M. Shaterloo, Chemical composition and antioxidant properties of γ-irradiated Iranian *Zataria multiflora* extracts. Pharm. Biol. **50**, 232–238 (2012). https://doi.org/10.3109/13880209.2011.596208
47. S.H. Pourhosseini, M.H. Mirjalili, M. Ghasemi, H. Ahadi, H. Esmaeili, M. Ghorbanpour, Diversity of phytochemical components and biological activities in *Zataria multiflora* Boiss. (Lamiaceae) populations. S. Afr. J. Bot. **135**, 148–157 (2020). https://doi.org/10.1016/j.sajb.2020.08.024
48. A.F. El-Yazbi, N.E. Elashkar, K.M. Abdel-Hay, W. Talaat, H.M. Ahmed, Eco-friendly HPTLC method for simultaneous analysis of sofosbuvir and ledipasvir in biological and pharmaceutical samples: stability indicating study. Microchem. J. **154**, 104584 (2020). https://doi.org/10.1016/j.microc.2019.104584
49. P. Izadiyan, A. Salehi, A. Moaddeli, M. Zarenezhad, M. Izadiyan, How quantity of bioactive compounds of *Zataria multiflora* differ using traditional or modern extraction methods. J. Med. Plants Byprod. **11**, 107–115 (2022). https://doi.org/10.22092/jmpb.2021.353668.1339
50. S. Teepoo, P. Dawan, N. Barnthip, Electrospun chitosan-gelatin biopolymer composite nanofibers for horseradish peroxidase immobilization in a hydrogen peroxide biosensor. Biosensors **7**, 47 (2017). https://doi.org/10.3390/bios7040047
51. K. Kalantari, A.M. Afifi, H. Jahangirian, T.J. Webster, Biomedical applications of chitosan electrospun nanofibers as a green polymer—review. Carbohydr. Polym. **207**, 588–600 (2019). https://doi.org/10.1016/j.carbpol.2018.12.011
52. S. Wang, G. Zhao, Quantitative characterization of the electrospun gelatin–chitosan nanofibers by coupling scanning electron microscopy and atomic force microscopy. Mater. Lett. **79**, 14–17 (2012). https://doi.org/10.1016/j.matlet.2012.03.044
53. A. Pangon, S. Saesoo, N. Saengkrit, U. Ruktanonchai, V. Intasanta, Hydroxyapatite-hybridized chitosan/chitin whisker bionanocomposite fibers for bone tissue engineering applications. Carbohydr. Polym. **144**, 419–427 (2016). https://doi.org/10.1016/j.carbpol.2016.02.053
54. B.C. Geiger, M.T. Nelson, H.R. Munj, D.L. Tomasko, J.J. Lannutti, Dual drug release from CO_2-infused nanofibers via hydrophobic and hydrophilic interactions. J. Appl. Polym. Sci. (2015). https://doi.org/10.1002/app.42571
55. W. Tighzert, A. Habi, A. Ajji, T. Sadoun, F.B.-O. Daoud, Fabrication and characterization of nanofibers based on poly(lactic acid)/chitosan blends by electrospinning and their functionalization with phospholipase A1. Fibers Polym. **18**, 514–524 (2017). https://doi.org/10.1007/s12221-017-6953-x
56. D. Babadi, S. Dadashzadeh, Z. Shahsavari, S. Shahhosseini, T.L.M. Ten Hagen, A. Haeri, Piperine-loaded electrospun nanofibers, an implantable anticancer controlled delivery system for postsurgical breast cancer treatment. Int. J. Pharm. **624**, 121990 (2022). https://doi.org/10.1016/j.ijpharm.2022.121990
57. A.H. Tayeb, M. Tajvidi, Sustainable barrier system via self-assembly of colloidal montmorillonite and cross-linking resins on nanocellulose interfaces. ACS Appl. Mater. Interfaces **11**, 1604–1615 (2019). https://doi.org/10.1021/acsami.8b16659
58. S. Ediyilyam, B. George, S.S. Shankar, T.T. Dennis, S. Wacławek, M. Černík, V.V.T. Padil, Chitosan/gelatin/silver nanoparticles composites films for biodegradable food packaging applications. Polymers **13**, 1680 (2021). https://doi.org/10.3390/polym13111680
59. L. Sharma, H.K. Sharma, C.S. Saini, Edible films developed from carboxylic acid cross-linked sesame protein isolate: barrier, mechanical, thermal, crystalline and morphological properties. J. Food Sci. Technol. **55**, 532–539 (2018). https://doi.org/10.1007/s13197-017-2962-4
60. I.M. Lipatova, A.A. Yusova, Effect of mechanical activation on starch crosslinking with citric acid. Int. J. Biol. Macromol. **185**, 688–695 (2021). https://doi.org/10.1016/j.ijbiomac.2021.06.139
61. P. Guerrero, A. Muxika, I. Zarandona, K. de la Caba, Crosslinking of chitosan films processed by compression molding. Carbohydr. Polym. **206**, 820–826 (2019). https://doi.org/10.1016/j.carbpol.2018.11.064
62. Y. Jiang, D. Ma, T. Ji, D.E. Sameen, S. Ahmed, S. Li, Y. Liu, Long-term antibacterial effect of electrospun polyvinyl alcohol/polyacrylate sodium nanofiber containing nisin-loaded nanoparticles. Nanomaterials (Basel) (2020). https://doi.org/10.3390/nano10091803
63. P. Shao, Y. Liu, C. Ritzoulis, B. Niu, Preparation of zein nanofibers with cinnamaldehyde encapsulated in surfactants at critical

micelle concentration for active food packaging. Food Packag. Shelf Life **22**, 100385 (2019). https://doi.org/10.1016/j.fpsl.2019.100385